The effects of 3d alloying elements on grain boundary cohesion in γ-iron: a first principles study on interface embrittlement due to the segregation

2003 J. Phys.: Condens. Matter 15 8339

(http://iopscience.iop.org/0953-8984/15/49/012)

INSTITUTE OF PHYSICS PUBLISHING JOURNAL OF PHYSICS: CONDENSED MATTER

J. Phys.: Condens. Matter **15** (2003) 8339–8349 PII: S0953-8984(03)66327-7

The effects of 3d alloying elements on grain boundary cohesion in γ-iron: a first principles study on interface embrittlement due to the segregation

R Yang[1], R Z Huang[1], Y M Wang[1,3], H Q Ye[1] and C Y Wang[2]

[1] Shenyang National Laboratory for Materials Science, Institute of Metal Research, Chinese Academy of Sciences, 72 Wenhua Road, Shenyang 110016, People's Republic of China
[2] Central Iron and Steel Research Institute, No 13 Taipingzhuang Outside Xizhimen, Beijing, People's Republic of China

E-mail: ymwang@imr.ac.cn

Received 16 July 2003
Published 25 November 2003
Online at stacks.iop.org/JPhysCM/15/8339

Abstract

By the use of a first principles density functional theory, two kinds of models, namely the Rice–Wang thermodynamics model and the Seah quasi-chemical model, are employed to evaluate the embrittling tendency of a grain boundary (GB) due to the 3d element segregation. The first principles method based on those two models is appropriate for calculating the chemical and structural relaxation contributions to the changes of GB cohesion with the 3d segregants. The effects of the 3d transition elements, such as Ti, V, Cr and Mn, on a stable fcc Fe $\Sigma 11[1\bar{1}0]/(11\bar{3})$ GB are studied and the difference between these two models is interpreted. When the chemical and the structural relaxation effects are taken into account, the calculated results for these two models are coincident for most of the elements studied, except for chromium. After analysing their chemical bonding in detail, we find that this discrepancy may be attributable to a lower susceptibility of the Seah model to the bonding anisotropy caused by Cr in the GB. It is proposed that the Seah model should be prudently used for some elements, especially those lying in the middle of a transition period.

1. Introduction

A central task of theoretical and experimental studies of interface segregation is to understand the behaviour of solute atoms on atomic cohesion at an interface [1]. A number of theories and mechanisms have been proposed to describe the segregation-induced modifications to the cohesion of grain boundaries (GBs) [2–4]. Mclean [5] has given the ideal work of fracture of a clean GB, γ^0, [5] as

[3] Author to whom any correspondence should be addressed.

0953-8984/03/498339+11$30.00

$$\gamma^0 = 2\gamma_s^0 - \gamma_b^0, \tag{1}$$

where γ_s^0 and γ_b^0 are the surface energies of a clean fracture and a clean GB respectively. Based on Mclean's work, many models have been proposed to describe the effect of segregants so far.

Stark and Marcus [6] devised two models for calculating the segregation energy of GB required for an intergranular fracture by the cohesive energies of the segregant and host element. They found that the segregant with a much smaller cohesive energy than that of the host element would give rise to an easy boundary separation. In a similar way, Seah proposed a theory to account for the effect of segregants on the GB cohesion [7], in which the brittle behaviour of a GB was evaluated by using the pair-bonding or quasi-chemical approach. By counting up the number of dangling bonds crossing the GB atoms per unit area and then summing their energies, the actual energy required to break those bonds in a fracture process was determined. For a binary system with solute B in solvent A, when the nearest neighbour bond energies ε_{AA}, ε_{AB} and ε_{BB} are assigned to AA, AB and BB neighbours, respectively, the fracture energy, FE(0), of pure solvent, and the fracture energy, FE(X_b), with a molar fractional monolayer of solute B, X_b, at the GB is given as

$$\mathrm{FE}(0) = -\left(\frac{Z_g}{a_A^2}\right)\varepsilon_{AA}, \tag{2}$$

$$\mathrm{FE}(X_b) = -\frac{Z_g}{a_A^2}\left\{\left(1 - \frac{1}{2}X_b\right)^2 \varepsilon_{AA} + X_b\left(1 - \frac{1}{2}X_b\right)\varepsilon_{AB} + \frac{1}{4}X_b^2\varepsilon_{BB}\right\}, \tag{3}$$

where Z_g, as described by Seah, is the coordination of atoms in a layer on one side of the GB to those in the adjacent layer on the other side, and a_A is the atom size of A.

If the AB system is an ideal solution,

$$\varepsilon_{AB} = \tfrac{1}{2}(\varepsilon_{AA} + \varepsilon_{BB}). \tag{4}$$

And if A and B have different sizes, the reduction in fracture energy induced by segregation may be approximately written as

$$\mathrm{FE}(0) - \mathrm{FE}(X_b) = -\frac{X_b Z_g}{2}\left(\frac{\varepsilon_{BB}}{a_B^2} - \frac{\varepsilon_{AA}}{a_A^2}\right), \tag{5}$$

where X_b is the fractional area of the GB covered by B atoms, and a_B is the atomic size of B.

In order to determine the value of ε_{AA} and ε_{BB}, the molar sublimation enthalpies, H^{sub}, are introduced. Therefore the final form of equation (5) can be written as

$$\mathrm{FE}(0) - \mathrm{FE}(X_b) = -\frac{X_b Z_g}{Z}(H_A^{sub^*} - H_B^{sub^*}), \tag{6}$$

where $H_{A\text{ or }B}^{sub^*}$ represents the sublimation enthalpy of pure A or B per unit area derived from

$$H^{sub^*} = H^{sub}/Na^2, \tag{7}$$

where N is Avogadro's number, and a is the atomic radius of A or B.

The numerical calculation of equation (6) allows one to plot a distribution scheme of embrittling and remedial segregants on their H^{sub^*} in any solvent matrix, as plotted by Seah for the iron matrix in figure 1. In this scheme, taking any given element as the matrix, elements having lower H^{sub^*} than it would, if segregated, cause the interface embrittlement of the matrix, whereas elements with higher H^{sub^*} than it would remedy such embrittlement. This scheme is accessible for evaluating the embrittlement trend of a GB. Thus the Seah model has been widely used in studies of material structure and properties.

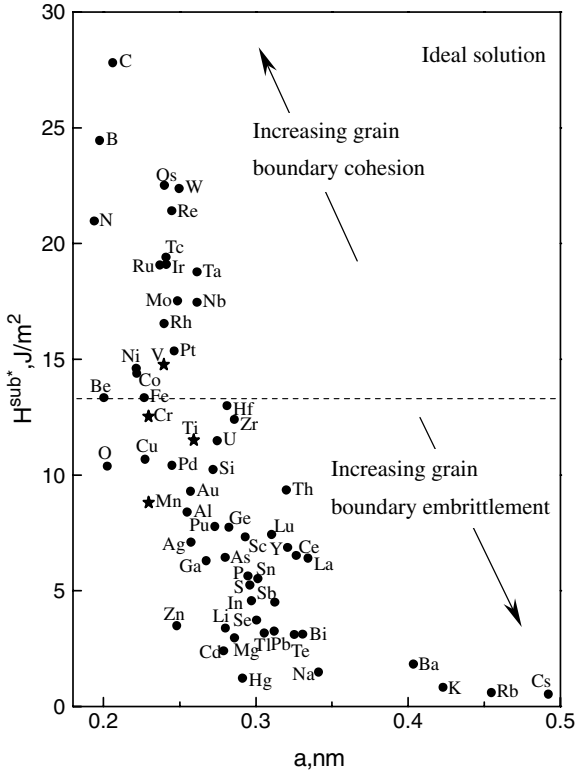

Figure 1. The general embrittlement–remedial element distribution plot in an iron matrix with an ideal solution approximation, given by Seah [7]. The dashed line through Fe divides these elements as segregant into two parts; those above the line increase GB cohesion but those below the line reduce it.

According to the segregation thermodynamics, an alternative model for analysing the ideal work of fracture of segregated GBs, γ, was made by Hirth and Rice [8]. The reduction in the ideal work of fracture, during which there is no redistribution of segregant species to be supposed, is given by

$$\gamma \cong \gamma^0 - \int_0^{\Gamma_b} [\mu_b(\Gamma) - \mu_s(\Gamma/2)]\, d\Gamma, \tag{8}$$

where $\mu_b(\Gamma)$ and $\mu_s(\Gamma)$ are the chemical potentials of the solute species in equilibrium with a level segregation Γ mol m^{-2} at the GB and the free surface (FS) respectively.

Within the dilute solute concentration limits, this relation was re-expressed by Rice and Wang as follows [9]:

$$\gamma \cong \gamma^0 - (\Delta g_b - \Delta g_s)\Gamma, \tag{9}$$

where Δg_b and Δg_s are the Gibbs free energies of a GB and a FS due to the solute segregation, respectively. In the case of $\Delta g_b - \Delta g_s < 0$, the solute atoms tend to segregate to a GB comparing with a FS, that is, the brittle tendency of interface separation would be reduced, while their positive difference means that the solutes tend to segregate to a surface and thus would reduce the GB cohesion. A modified Rice–Wang model by using a first principles method makes it possible to study the embrittling trend of segregants, which provides a powerful tool to evaluate the GB properties and a convenient way to detail the segregation behaviour.

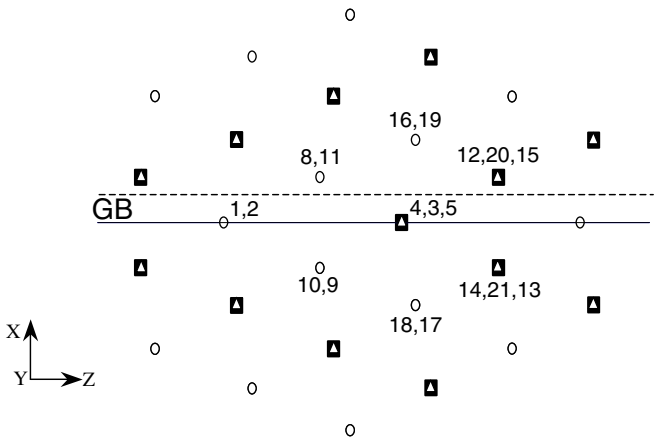

Figure 2. The atomic cluster around $\Sigma 11[1\bar{1}0]/(11\bar{3})$ tilt GB in γ-iron. ■, ○ and △ represent atoms in the different X–Z layers. The *y* axis is denoted by Y and runs in the perpendicular direction to the paper plane. Some atoms in the cluster are labelled by the numbers near the symbol. The alloying element M, such as Ti, V, Cr and Mn, substitutes for the Fe3 atom in the GB plane. The dash line denotes the separate plane during the fracture.

In this paper, we focus on the effects of 3d transition-metal alloying elements M (M = Ti, V, Cr and Mn) on the cohesion of a γ-iron $\Sigma 11[1\bar{1}0]/(11\bar{3})$ GB by performing the first principles calculations as will be described in section 2. In section 2 we will present an atomic model and describe the computational details. The calculated results of segregation energies for different systems will be given in section 3 and discussed in section 4. Our summaries will be given in the last section.

2. Model and computation details

A cluster model simulating the γ-iron $\Sigma 11[1\bar{1}0]/(11\bar{3})$ tilt GB was constructed as shown in figure 2, which contains 67 Fe atoms. This model can be used to estimate the segregation effects of 3d alloying elements by each of them substituting for the Fe3 atom in the γ-iron GB independently. The primary clean Fe GB was created by using a coincidence site lattice (CSL) model and then relaxing to obtain the stable configuration by using molecular dynamics (MD) and total energy minimization methods.

In the MD calculation, we employed the Murrell–Mottram many-body potential [10], which is an empirical potential generally used for modelling solids, surfaces and clusters. The effective potential can be obtained by fitting experimental data, such as lattice energies, lattice constants, vacancy formation energies, phonon dispersion curves and elastic constants etc. To test the validity of the potential obtained for fcc Fe, we have performed an MD calculation for an fcc Fe bulk model containing 6912 atoms. The calculated lattice constant of fcc Fe is 0.362 nm, which agrees well with the experimental value of 0.368 nm (extrapolated to 1428 K). The bulk modulus is 89 GPa, the two shear moduli $C' = (1/2)(C_{11} - C_{12}) = 73$ GPa and $C_{44} = 134$ GPa. All three elastic constants are positive. The cohesive energy per atom calculated by using the MD method is -5.86 eV for the pure fcc Fe GB model (containing 13 860 atoms), while it is -5.68 eV for the FS model. The difference between them is -0.18 eV, which is comparable with the difference of -0.18 eV between -4.95 eV for pure Fe GB and -4.77 eV for FS obtained by our first principles calculation. Thus we can have a stronger confidence in the constructed GB configuration in this paper.

In fact, it shows that there is less atomic displacement from the CLS sites including about 13 860 atoms after the MD relaxation, which means that the CSL model is a good approximation for the pure Fe $\Sigma 11[1\bar{1}0]/(11\bar{3})$ GB. After the relaxation, a smaller GB cluster model (67 atoms) large enough to contain more than one GB periodic unit was selected from the MD relaxation model. To obtain the total energy minimization configurations of the segregation GB models we also performed a first principles relaxation within the limits of the GB symmetry.

To consider sufficiently the influence of environment of FE atoms, the GB and surface atomic models were embedded in 908 and 463 circumstance Fe atoms respectively, which were used to be the pseudo-potentials in the embedded cluster technique.

Based on the Rice–Wang thermodynamics model, some first principles calculations gave an easy numerical evaluation of the fracture behaviour due to the GB segregation of the alloying elements [11–18]. However, most of these studies only indicated the resultant effect of the segregants but did not explore their effects during fracture. In fact, in many cases, just those effects could provide a clear understanding of the segregation behaviour. This is the main concern of this paper.

In order to study conveniently the chemical and structure relaxation contributions to the cohesion of a GB, we assume that a fracture process may be divided into two stages. Firstly, the GB may be detached into two separate surfaces (SSs) without any relaxation, and then the SSs may be relaxed into free surfaces (FSs). This means physically that the actual energy required to separate a GB with or without solute segregation is determined not only by the energy needed to break the bonds across the GB (chemical effect) but also by the energy required to relax just separated surfaces (structural relaxation effect).

The segregation energy of solute atoms towards a GB, SS or FS can be written, respectively, as follows:

$$\Delta E_{\mathrm{GB}} = \frac{1}{M}(E^{\mathrm{b}}_{\mathrm{GB}+M} - E^{\mathrm{b}}_{\mathrm{GB}}), \tag{10}$$

$$\Delta E_{\mathrm{FS}} = \frac{1}{M}(E^{\mathrm{b}}_{\mathrm{FS}+M} - E^{\mathrm{b}}_{\mathrm{FS}}), \tag{11}$$

$$\Delta E_{\mathrm{SS}} = \frac{1}{M}(E^{\mathrm{b}}_{\mathrm{SS}+M} - E^{\mathrm{b}}_{\mathrm{SS}}), \tag{12}$$

where E^{b}_{*+M}, E^{b}_{*} ($* =$ GB, SS or FS) is the binding energy of $*$ with or without the segregants, respectively. M is the solute molar fraction. Therefore, the chemical effect of solute segregation on the fracture energy can be described by $\Delta E_{\mathrm{GB}} - \Delta E_{\mathrm{SS}}$ and the structural relaxation effect by $\Delta E_{\mathrm{SS}} - \Delta E_{\mathrm{FS}}$. Ignoring the entropy terms, $\Delta g_{\mathrm{b}} - \Delta g_{\mathrm{s}}$ in equation (9) is equivalent to $\Delta E_{\mathrm{GB}} - \Delta E_{\mathrm{FS}}$. Equation (9) has been applied successfully for studying the cohesion of both substituted and interstitial segregation GBs [19–21].

ΔE_{GB}, ΔE_{SS} and ΔE_{FS} can be determined by using a quantum mechanical calculation, which is able to give the precise energy on the atomic level. In this paper we used the discrete variational method (DVM) [22–25] based on density functional theory to investigate the segregation effects of 3d elements. The Von Barth and Hedin exchange–correction potential [26] was adopted, and atomic orbitals including 1s, 2s, 2p, 3s, 3p, 3d, 4s, 4p were used for Ti, V, Cr, Mn and Fe during the calculation. The matrix elements of the Hamiltonian and the overlap integrals were calculated by a discrete sampling method [27]. Over 70 000 spatial integration points are employed to calculate the potential and molecular orbital.

The bond order, $\mathrm{BO}_{\upsilon\upsilon'}$, between two atoms, which can be evaluated by Mulliken population analysis [28], is defined as

$$\mathrm{BO}_{\upsilon\upsilon'} = \sum_{l} n_l \sum_{ij} C^{\upsilon}_{il} C^{\upsilon'}_{jl} \int \Psi^{\upsilon}_{i} \Psi^{\upsilon'*}_{j} \,\mathrm{d}V, \tag{13}$$

Table 1. The calculated segregation energies (in eV) of GB, SS and FS for Ti/Fe, V/Fe, Cr/Fe and Mn/Fe GBs together with their difference.

	ΔE_{GB}	ΔE_{SS}	ΔE_{FS}	$\Delta E_{GB} - \Delta E_{SS}$	$\Delta E_{GB} - \Delta E_{FS}$
Ti/Fe GB	−1.78	−0.77	−2.19	−1.01	0.41
V/Fe GB	−2.12	−0.63	−1.50	−1.49	−0.63
Cr/Fe GB	−4.77	−2.25	−3.67	−2.52	−1.10
Mn/Fe GB	−0.98	−0.40	−3.03	−0.58	2.05

where Ψ_i^{υ} and $\Psi_j^{\upsilon'}$ are the respective wavefunctions of the i and j orbitals of atoms υ and υ'. C_{il}^{υ} and $C_{il}^{\upsilon'}$ are coefficients, whose product shows the magnitude of the linear combination of atomic orbitals in the molecular orbital l. n_l is the occupied charge of the molecular orbital l. The bond order can be used to evaluate the strength of the covalent-like bonding between two atoms.

The crystal orbital overlap population (COOP) can be used to measure the orbital overlap degree of different atoms in an energy interval [29, 30]. The bond overlap population (BOP) is obtained by integrating the corresponding COOP up to the Fermi energy (E_F), which can be used to evaluate the orbital interaction.

3. Results

3.1. Segregation energy

In the GB relaxed by using the first principles method, the 3d atom slightly pushes its first and second neighbouring Fe atoms such as Fe4, Fe5, Fe8–Fe11 away from it, but keeps Fe16–Fe19 atoms unmoved. These relaxation results are consistent with those from Zhong *et al* [31] by using FLAPW method, who found that the substitutive Mn on the bcc Fe GB would slightly push its neighbourhood Fe atoms outwards.

The calculated segregation energies for GB, SS and FS are listed in table 1. From table 1, all the values of $\Delta E_{GB} - \Delta E_{SS}$ for the Fe GBs with 3d element segregants are negative; this means an increase in fracture energy of the GB, proportional to the corresponding value of $\Delta E_{GB} - \Delta E_{SS}$. If only the chemical effect of 3d alloying elements is considered, it seems that these elements attempt to improve the Fe GB cohesion. For example, the Fe GB with Cr ($\Delta E_{GB}^0 - \Delta E_{SS}^0 = -2.52$ eV) may be more cohesive than that with Mn (−0.58 eV).

In comparison with the values of $\Delta E_{GB}^0 - \Delta E_{SS}^0$, the values of $\Delta E_{SS}^0 - \Delta E_{FS}^0$ are all positive; this means a decrease in fracture energy of the GB, caused by the structural relaxation effect, which is proportional to the corresponding value of $\Delta E_{SS}^0 - \Delta E_{FS}^0$. Combining the chemical effect beneficial to the Fe GB cohesion with the structural relaxation effect detrimental to it, i.e. the values of $\Delta E_{GB}^0 - \Delta E_{FS}^0$ listed in table 1, one can find that the 3d elements V and Cr may increase the GB cohesion but Ti and Mn may detract from it. Among them, Cr has a stronger beneficial effect on enhancing the cohesion of the GB than V, while Mn is a more powerful embrittling element than Ti. Most of DVM results for 3d elements agree well with those in figure 1 predicted by Seah except for Cr, which was predicted by Seah as an element to facilitate the brittle fracture of the Fe GB. The discrepancy between Seah's prediction and our calculation result for Cr demonstrates clearly that there is a necessity to consider the chemical effect of doping atoms and their structural relaxation effect on the cohesion of a GB rather than only the bonding across the GB as done by Seah.

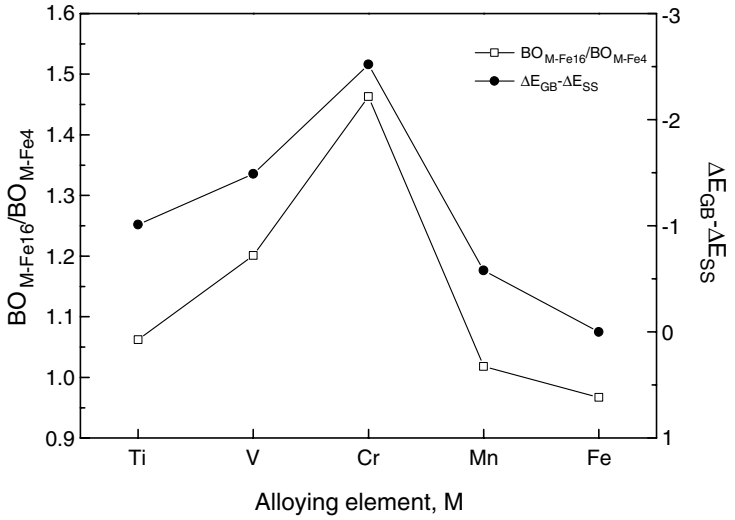

Figure 3. The dependence of the ratio of BO_{M-Fe16}/BO_{M-Fe4} and the segregation energy difference $\Delta E_{GB} - \Delta E_{SS}$ on the alloying segregant M.

Table 2. The atomic bond order between atoms in different GBs.

Atomic Pairs	Ti/Fe GB	V/Fe GB	Cr/Fe GB	Mn/Fe GB	Clean Fe GB
Vertical plane					
Fe9–Fe11	0.443	0.443	0.423	0.431	0.424
Fe21–Fe20	0.383	0.367	0.348	0.350	0.348
Fe13–Fe15	0.516	0.518	0.520	0.517	0.519
Fe3(Mn, Cr)–Fe16	0.273	0.292	0.294	0.279	0.267
Lying plane					
Fe9–Fe10	0.259	0.243	0.280	0.255	0.260
Fe3(Mn, Cr)–Fe4	0.257	0.243	0.201	0.274	0.276

3.2. Bond order

The atomic bond orders in different GBs are listed in table 2. In table 2, M/Fe GB (M = Ti, V, Cr, and Mn) denotes such a GB, where M substitutes for the Fe atom in the clean Fe GB.

In the clean Fe GB, the interactions between Fe3 and the Fe atoms surrounding it, such as Fe3, Fe5 and Fe16–19, are almost equal, presenting an isotropic bonding. However, the substitution of M for Fe3 can strengthen the bonds in the vertical direction to the GB plane, for example, M–Fe16–19 bonds, but weaken those on the GB plane, such as M–Fe4 and M–Fe5 bonds. This kind of anisotropy in bonding due to the M substitution would be in favour of strengthening the GB.

For explicitly revealing the relationship between the bonding anisotropy and GB cohesion, the bond order ratio of BO_{M-Fe16} to BO_{M-Fe4} together with the chemical effect of M on GB cohesion, i.e. $\Delta E_{GB} - \Delta E_{SS}$, is plotted in figure 3. It can be found that the bond order ratio increases with M in the sequence of Ti, V and Cr and then reduces at Mn. For the clean Fe GB, it is approximately unity. A similar variant trend of the bond order ratio versus M to the value of $\Delta E_{GB} - \Delta E_{SS}$ versus M demonstrates clearly that the effect of M on strengthening the GB cohesion mainly comes from its bonding anisotropy rather than only from the bonding strength between two atoms.

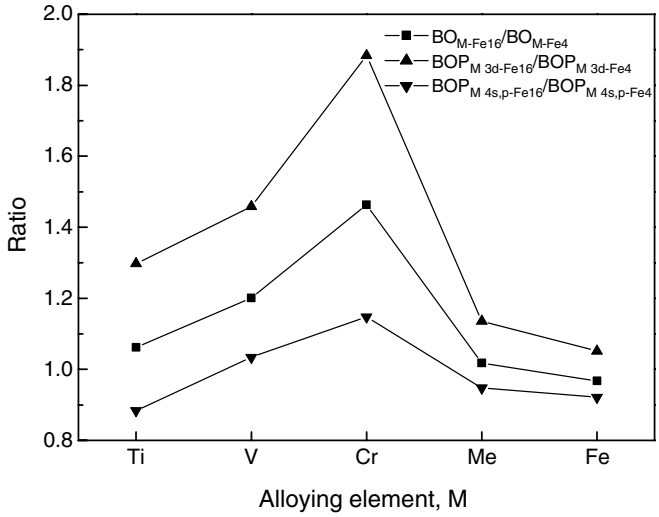

Figure 4. The dependence of the ratio of BO_{M-Fe16}/BO_{M-Fe4}, $BO_{M\,3d-Fe16}/BO_{M\,3d-Fe4}$ and $BO_{M\,4s,p-Fe16}/BO_{M\,4s,p-Fe4}$ on the alloying segregant M.

To understand this kind of the boding anisotropy more deeply, we calculate the dependence of the ratios of the atomic bond order, BO_{M-Fe16}/BO_{M-Fe4}, the 3d and 4s, p orbital interactions, $BOP_{M\,3d-Fe16}/BOP_{M\,3d-Fe4}$ and $BOP_{M\,4s,p-Fe16}/BOP_{M\,4s,p-Fe4}$, on M as shown in figure 4. The higher the ratio is, the stronger the bonding is in the vertical direction compared with that in the horizontal direction on the GB plane. As shown in figure 4, the ratios of the 3d and 4s, p orbital interactions have a similar trend with M. However, the 3d orbital interaction ratio is larger than the corresponding 4s, p one, especially for Cr. Therefore, it would be reasonable to conclude that this kind of bonding anisotropy of 3d transition elements may mainly come from their d orbital interaction.

3.3. Density of state (DOS) and crystal orbital overlap population (COOP)

For further understanding the bonding characteristic of M (or Fe3)–Fe4 and M (or Fe3)–Fe16 bonds, the 3d and 4s, p partial density of state (PDOS) and their COOP curves are calculated and shown in figure 5. The Fermi energy level is set as zero. It can be seen from figures 5(c) and (d) that the essential parts of the DOSs of Fe4 and Fe16 lie below but near E_F. The main difference between them is that Fe16 DOS has an extra 3d parcel below E_F and its essential part overlaps over M (or Fe3) 3d DOS. The M 3d PDOS, comparing with the 4s, p PDOS, is evidently shifted to a lower energy region with the increased atomic number of M as shown in figures 5(a) and (b) but the DOS curves of Fe4 and Fe16 are almost invariable with M. As a result of its shift, the M (or Fe3) 3d–Fe16 bonding interaction, which can be measured by the area under the corresponding COOP curve below E_F in figure 5(g), becomes stronger than that of M (or Fe3) 3d–Fe4, as shown in figure 5(e). However, in the case of Mn/Fe and pure Fe GB, because the anti-bonding parts of their corresponding COOP curves below E_F are larger than other COOP curves, the ratios of the 3d orbital interactions would be smaller due to this kind of interaction being reduced. In summary, the beneficial bonding anisotropy due to the substitution of M for Fe3 would increase with M from Ti to Cr and then decrease from Cr to Fe as has been shown in figure 4. In addition, the kind of anisotropy is mainly caused by the d orbital interaction because the COOP curves of $M_{4s,p}$–Fe4 and $M_{4s,p}$–Fe16 below E_F change little with M.

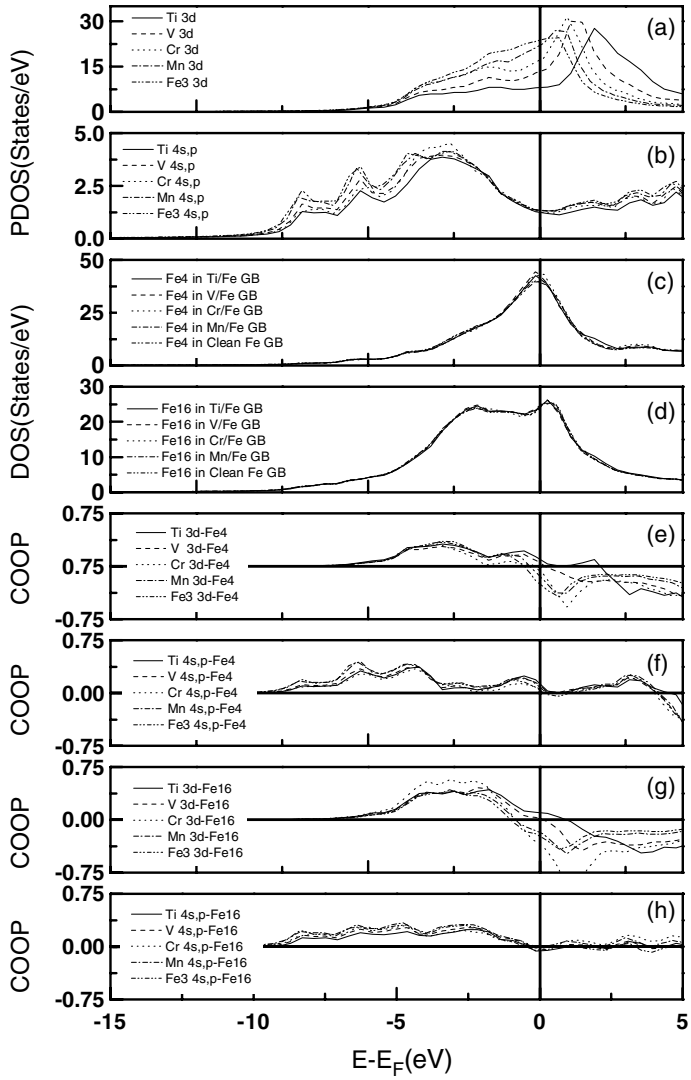

Figure 5. The PDOS curves for M (M = Ti, V, Cr, Mn and Fe) at the Fe3 site DOS curves of Fe4 and Fe16 atoms together with the COOP curves between the M–Fe4 bond and M–Fe16 bonds. (a) 3d PDOS of M; (b) 4s, p PDOS of M; (c) DOS of Fe4; (d) DOS of Fe16; (e) COOP of M 3d–Fe4; (f) COOP of M 4s, p–Fe4; (g) COOP of M 3d–Fe16 and (h) COOP of M 4s, p–Fe16.

4. Discussions

It could be concluded from the above calculations and analysis that the 3d orbital interaction of M at the Fe3 site is mainly responsible for the bonding anisotropy. For 3d elements in the middle of a transitional period, such as Cr, this effect is much stronger. This is because there are the maximum number of half-filled d orbitals and a weaker screen effect of the outer 4s, p orbital on them. For example, Cr has five half-filled d orbitals but only one filled 4s orbital. As the result of such molecular orbital structure, these middle elements would present the stronger bonding anisotropy. In fact, the competition of the beneficial effect due to the

bonding anisotropy with the detrimental structural relaxation effect will determine the resultant GB cohesion.

The detrimental structural relaxation effect during fracture depends closely on the atomic volume difference between a substitutive and an atom being substituted. The larger the substitutive atom, the more the embrittling of the GB because of it giving rise to an intense strain field [32, 33]. However, the stronger bonds between the substitutive M and the Fe atoms surrounding it would restrict the relaxation of atoms in the GB and therefore make it difficult to create two strain-free surfaces. The weaker structural relaxation effect of Cr and V than Ti and Mn is due to their smaller atomic radii, and their stronger chemical effect than Ti and Mn is due to the stronger bonding with the surrounding Fe atoms in the GB.

Previous studies of the effect of bonding anisotropy on enhancing GB cohesion [15–17] have pointed out that some impurities in a GB with the stronger bonding in the vertical direction compared with the horizontal direction of a GB plane may be favourable to enhance the cohesion of the GB, such as boron in Fe GB.

Physically, such a cohesion enhancement due to the bonding anisotropy is easily understood. Firstly, a GB cohesion is mainly determined by those bonds across the GB plane. The stronger the bonds in the vertical to the GB plane, numerically the smaller (or more negative) the value of $\Delta E_{\mathrm{GB}} - \Delta E_{\mathrm{SS}}$, the more cohesive the GB. Secondly, the increment of bonding charge on a GB plane will increase its activity and thus increase the free energy of two surfaces generated from the GB plane during fracture [34]. In other words, the lower bonding charge on a GB plane will decrease the surface energy and thus reduce the value of $\Delta E_{\mathrm{GB}} - \Delta E_{\mathrm{SS}}$. The present calculations find that either $\Delta E_{\mathrm{GB}} - \Delta E_{\mathrm{SS}}$ or $\Delta E_{\mathrm{SS}} - \Delta E_{\mathrm{FS}}$ is susceptible to the bonding anisotropy.

Equation (6) from the Seah model based on the pair bonding or quasi-chemical approach allows us to easily but qualitatively evaluate the embrittling trend of segregant to a host GB. However, this model treated the interaction between two atoms too simply to reflect their bonding anisotropy. In the case of a weaker bonding anisotropy, such as Ti, Mn and V in Fe GB, the Seah model will give coincident results with the Rice–Wang model. But when there is a stronger bonding anisotropy, a serious deviation between the calculated and true fracture energies would appear for the Seah model, such as Cr in an Fe GB. This means that one is unable to use the Seah model for such a case.

5. Summary

The Rice–Wang thermodynamics and Seah quasi-chemical models, which are widely used to evaluate the interface embrittlement due to segregations, have been carefully compared by using a first principles density functional method. For this comparison, the effects of 3d alloying elements on the cohesion of the γ-iron $\Sigma 11[1\bar{1}0]/(11\bar{3})$ GB have been calculated. Both the models afford almost the same results for such alloying elements with a weaker anisotropic bonding with surrounding atoms. However, for some elements presenting a stronger bonding anisotropy, a serious discrepancy between the two models will appear. The first principles density functional calculation results based on the Rice–Wang model may well present the effect of such bonding anisotropy on the interface embrittlement, but those based on the Seah model may not do so due to its lower sensibility to the bonding anisotropy. It is proposed that the Seah model should be carefully used in the segregation case of those transition elements lying in the middle of a transition period.

We should emphasize that although fcc iron is antiferromagnetic [35], the present calculations do not include any magnetic effects. Therefore, it may be expected that the calculated energies of GB cohesion are somewhat different from the true ones.

Acknowledgments

We acknowledge financial support of this work by the National Natural Science Foundation of China under the grant No. 50271071 and by the Special Funds for the Major State Basic Research Projects of China under the grant number of G2000067104.

References

[1] Wolfgang L 1979 *Acta Metall.* **27** 1885
[2] Cottrell A H 1990 *Meas. Sci. Technol.* **6** 121
[3] Cottrell A H 1990 *Meas. Sci. Technol.* **6** 325
[4] Hondros E D, Seah M P, Hofmann S and Lejek P 1996 *Physical Metallurgy* 4th revised and enhanced edn (Amsterdam: Elsevier Science BV) chapter 13 (Interfacical and Surface Microchemistry)
[5] Mclean D 1957 *Grain Boundaries in Metals* (Oxford: Oxford University Press)
[6] Stark J P and Marcus H L 1977 *Metall. Trans.* A **8** 1423
[7] Seah M P 1980 *Acta Metall.* **28** 955
[8] Hirth J P and Rice J R 1980 *Metall. Trans.* A **11** 1501
[9] Rice J R and Wang J S 1989 *Mater. Sci. Eng.* A **107** 23
[10] Cox H, Johnston R L and Murrell J N 1999 *J. Solid State Chem.* **145** 517
[11] Wu R Q, Freeman A J and Olson G B 1994 *Phys. Rev.* B **50** 75
[12] Wu R Q, Freeman A J and Olson G B 1992 *J. Mater. Res.* **7** 2433
[13] Tang S P, Freeman A J and Olson G B 1993 *Phys. Rev.* B **47** 2441
[14] Wu R Q, Freeman A J and Olson G B 1993 *Phys. Rev.* B **47** 6855
[15] Tang S P, Freeman A J and Olson G B 1994 *Phys. Rev.* B **50** 1
[16] Wu R Q, Freeman A J and Olson G B 1994 *Science* **265** 376
[17] Sagert L P, Oslon G B and Ellis D E 1998 *Phil. Mag.* B **77** 871
[18] Geng W T, Freeman A J, Wu R, Geller C B and Raynolds J E 1999 *Phys. Rev.* B **60** 7149
[19] Yang R, Zhao D L, Wang Y M, Wang S Q, Ye H Q and Wang C Y 2001 *Acta Mater.* **49** 1079
[20] Yang R, Wang Y M, Ye H Q and Wang C Y 2001 *J. Phys.: Condens. Matter* **13** 4485
[21] Yang R, Wang Y M, Huang R Z, Ye H Q and Wang C Y 2002 *Phys. Rev.* B **65** 094112
[22] Ellis D E and Painter G S 1970 *Phys. Rev.* B **2** 2887
[23] Averill F W and Ellis D E 1973 *J. Chem. Phys.* **59** 6413
[24] Ellis D E, Benesh G A and Bykom E 1977 *Phys. Rev.* B **16** 3308
[25] Delley B, Ellis D E and Freeman A J 1983 *Phys. Rev.* B **27** 2132
[26] Von Barth U and Hedin L 1972 *J. Phys.: Condens. Matter* **5** 1629
[27] Guenzburger D and Ellis D E 1992 *Phys. Rev.* B **46** 285
[28] Mulliken R S 1955 *J. Chem. Phys.* **23** 1833
[29] Hughbanks R and Hoffmann R 1983 *J. Am. Chem. Soc.* **105** 3528
[30] Wijeyesekera S D and Hoffmann R 1984 *Organometal* **3** 949
[31] Zhong L P, Wu R Q, Freeman A J and Oslon G B 1997 *Phys. Rev.* B **55** 11133
[32] Eberhart M E, Donovan M M, Maclaren J M and Clougherty D P 1991 *Prog. Surf. Sci.* **36** 1
[33] Messmer R P and Briant C L 1982 *Acta Metall.* **30** 457
[34] Seah M P 1975 *Surf. Sci.* **53** 168
[35] Sandratskii L M 1998 *Adv. Phys.* **47** 91